Mon. Not. R. Astron. Soc. **000**, 000–000 (0000) Printed 5 February 2008 (MN LATEX style file v2.2)

The satellite distribution of M31

A. W. McConnachie[1,2] & M. J. Irwin[1]
[1] *Institute of Astronomy, Madingley Road, Cambridge, CB3 0HA, U.K.*
[2] *Department of Physics and Astronomy, University of Victoria, Victoria, B.C. V8P 5C2, Canada*

5 February 2008

ABSTRACT
The spatial distribution of the Galactic satellite system plays an important role in Galactic dynamics and cosmology, where its successful reproduction is a key test of simulations of galaxy halo formation. Here, we examine its representative nature by conducting an analysis of the 3-dimensional spatial distribution of the M31 subgroup of galaxies, the next closest system to our own. We begin by a discussion of distance estimates and incompleteness concerns, before revisiting the question of membership of the M31 subgroup. We constrain this by consideration of the spatial and kinematic properties of the putative satellites. Comparison of the distribution of M31 and Galactic satellites relative to the galactic disks suggests that the Galactic system is probably modestly incomplete at low latitudes by $\simeq 20\,\%$. We find that the radial distribution of satellites around M31 is more extended than the Galactic subgroup; $50\,\%$ of the Galactic satellites are found within $\sim 100\,$kpc of the Galaxy, compared to $\sim 200\,$kpc for M31. We search for "ghostly streams" of satellites around M31, in the same way others have done for the Galaxy, and find several, including some which contain many of the dwarf spheroidal satellites. The lack of M31-centric kinematic data, however, means we are unable to probe whether these streams represent real physical associations. Finally, we find that the M31 satellites are asymmetrically distributed with respect to our line-of-sight to this object, so that the majority of its satellites are on its near side with respect to our line-of-sight. We quantify this result in terms of the offset between M31 and the centre of its satellite distribution, and find it to be significant at the $\sim 3\,\sigma$ level. We discuss possible explanations for this finding, and suggest that many of the M31 satellites may have been accreted only relatively recently. Alternatively, this anisotropy may be related to a similar result recently reported for the 2dFGRS, which would imply that the halo of M31 is not yet virialised. Until such time as a satisfactory explanation for this finding is presented, however, our results warn against treating the M31 subgroup as complete, unbiased and relaxed.

Key words: Local Group - galaxies: general - galaxies: dwarf - galaxies: haloes

1 INTRODUCTION

The Galactic satellite system consists of approximately a dozen galaxies. This is an order of magnitude less than the number of haloes predicted to exist as satellites from CDM simulations (e.g. Kauffmann et al. 1993), although this conflict is potentially resolved by suppressing star formation in some subset of dark matter haloes (e.g. Bullock et al. 2000). Successful reproduction of the Galactic satellite system, in terms of internal properties, frequency, and spatial properties, is considered an important test of cosmological galaxy formation models. In galactic dynamics, too, satellite populations play an important role. For example, Little & Tremaine (1987), Kochanek (1996), Wilkinson & Evans (1999), Evans & Wilkinson (2000) and Evans et al. (2000) have used the Galactic and M31 satellite systems to calculate the dynamical mass of the host galaxies.

Willman et al. (2004) have questioned whether the current census of Galactic satellites is complete, and suitable for use in the above ways. They conclude that several satellites are probably missing at low Galactic latitudes, and suggest that searches for Galactic satellites could be suffering from incompleteness issues at large Galactocentric distances. According to their study, these effects could have resulted in a factor of up to 3 discrepancy between the observed and actual number of Galactic satellites.

Around distant galaxies, a preference for satellites to lie along the minor axis of the host galaxy has been reported, implying a preference for polar orbits. This is the so-called Holmberg effect, first noted by Holmberg (1969) and later revisited by Zaritsky et al. (1997). However, recent results

from SDSS question these findings, and indicate a preference for orbits in the plane of the disk (Brainerd 2005). Knebe et al. (2004) suggest these anisotropies are the result of the accretion of satellites along filaments, leading to a preference for satellites to be observed along the major axis of the host halo and reflecting their initial infall onto the host galaxy. However, given the ambiguous and contradictory nature of the observational studies, the significance of this is not clear.

The Holmberg effect is not observed around nearby systems, but the Galactic satellite distribution is anisotropic. The LMC and SMC are on the opposite side of the sky to the Ursa Minor and Draco dwarf spheroidals (dSphs), on an almost polar great circle on the sky. On the same great circle lies the Magellanic Stream (Mathewson et al. 1974), a large trail of HI gas which has been stripped from the Magellanic Clouds. This correlation in position led Lynden-Bell (1976) to hypothesise that the LMC, SMC, Ursa Minor and Draco were once part of a "Greater Magellanic Cloud", which was torn apart in the gravitational potential of the Galaxy and condensed to form the latter two galaxies. The LMC and SMC are proposed to be the surviving remnant of this body.

At around the same time, Lynden-Bell (1982) noticed that the Fornax, Leo I, II and Sculptor dwarf galaxies all appeared to align in another polar great circle (the "FLS" stream), in a similar fashion to the Magellanic Stream. Later work by Majewski (1994) showed that the then newly discovered Sextans and Phoenix dwarf galaxies both aligned with this plane, along with most of the Galactic globular clusters with the reddest horizontal branches. Lynden-Bell & Lynden-Bell (1995) searched for all possible streams of satellites in the halo of the Galaxy, including some of the distant globular clusters, and found several candidates in addition to the Magellanic and FLS streams.

Kinematic evidence for these streams is still inconclusive. Only radial velocities can be measured readily and although some proper motions for these satellites exist, a common consensus has yet to emerge for most of the dSphs. For example, Schweitzer (1996) conclude that Ursa Minor appears consistent with it moving in the direction of the Magellanic Clouds, although a more recent measurement by Piatek et al. (2005) concludes that its membership of the Magellanic Stream is unlikely. Sculptor and Fornax have proper motion measurements consistent with their membership of the FLS stream (Schweitzer 1996; Dinescu et al. 2004), although an earlier measurement for Fornax had ruled out membership of this stream (Piatek et al. 2002).

Kroupa et al. (2005) have suggested that the distribution of Galactic satellites is inconsistent with the distribution of satellites expected from CDM simulations. Zentner et al. (2005), however, point out that a spherical distribution of satellites is not the correct null hypothesis for dealing with CDM simulations, and the results of Kroupa et al. (2005) are marginally consistent with a prolate distribution of satellites. Libeskind et al. (2005) find that the subset of subhaloes which have the most massive progenitors at early times, and therefore arguably the ones most likely to be luminous, are distributed in a similar way to the Galactic satellites, even though the overall distribution of dark matter and dark satellites is very different. In a similar way to Knebe et al. (2004), this result is interpreted in terms of the accretion of satellites along filaments.

The satellite distribution of the Galaxy therefore plays an important role in cosmology and galactic dynamics. Whether this distribution is representative of satellite systems in general still needs to be answered. As a result, the analysis of the spatial distribution of similar systems is important to several fields. We are currently involved in an extensive study of M31 and its environment (Ibata et al. 2001, 2004, 2005; Ferguson et al. 2002; McConnachie et al. 2003, 2004b,c, 2005; McConnachie & Irwin 2005b; Chapman et al. 2005; Irwin et al. 2005). This galaxy hosts the next closest satellite subsystem to our own and in this contribution we conduct an analysis of its spatial distribution and compare it to the Galactic satellites, to explore the uniqueness of our satellite system. Some of the results presented here have previously been discussed briefly in McConnachie et al. (2004a) and McConnachie & Irwin (2005a). In Section 2 we discuss the initial set of galaxies which we study, incompleteness concerns, and the distance measurements that we use for each. We also define a M31 spherical coordinate system, in analogy to Galactic coordinates. In Section 3, we use the distance and radial velocity data for the Local group galaxies to revisit the question of membership of the M31 subgroup. In Section 4 we analyse the spatial distribution of the satellite system and compare it with our own Milky Way. In Section 5, we search for "ghostly" streams around M31, in a similar way to Lynden-Bell & Lynden-Bell (1995). Section 6 discusses some of our findings, and Section 7 summarises.

2 THE DATA

Most Galactic satellites are located within some 200 kpc of the Sun. Distances to these objects are reliably determined, and are typically accurate to 5%. It is therefore relatively easy to conduct a reliable analysis of the distribution with respect to the Milky Way, as the data is of high quality and only a small correction needs to be applied to account for the offset of the Sun from the Galactic centre.

M31 is located at a distance of $\simeq$ 780 kpc (eg. Freedman & Madore 1990; Joshi et al. 2003; Brown et al. 2004; McConnachie et al. 2005). Some 14 to 18 other galaxies are believed to be associated with it at roughly equivalent heliocentric distances (of order $600 - 1000$ kpc). Accurate relative distances to each of these objects is crucial for a study of their distribution around M31, as the correction that must be applied to account for our offset from M31 is two orders of magnitude larger than for the Galactic centre. Additionally, it is important to have an understanding of any possible incompleteness in the dataset (ie. currently undiscovered group members). In this section, we first present the data that we will be using, and define a coordinate system in which to analyse them. We then discuss the accuracy of the data, and comment on incompleteness effects.

2.1 The Possible Members

A full list of all galaxies which are initially considered as possible members of the M31 subgroup are listed in Table 1, along with their Galactic coordinates, adopted distance and uncertainty, and radial velocity. For completeness, we start by considering all Local Group candidates in the same part

Galaxy	l	b	r (kpc)	$v_\odot$ (km s^{-1})
M31	121.2	-21.5	785 ± 25	-301
M33	133.6	-31.3	809 ± 24	-180
NGC 205	120.7	-21.7	824 ± 27	-244
NGC 147	119.8	-14.3	675 ± 27	-193
NGC 185	120.8	-14.5	616 ± 26	-202
And I	121.7	-24.9	745 ± 24	-380
And II	128.9	-29.2	652 ± 18	-188
And III	119.3	-26.2	749 ± 24	-355
And V	126.2	-15.1	774 ± 28	-403
And VI	106.0	-36.3	783 ± 25	-354
And VII	109.5	-9.9	763 ± 35	-307
And IX	123.2	-19.7	765 ± 24	-216
LGS3	126.8	-40.9	769 ± 23	-286
Pegasus	94.8	-43.5	919 ± 30	-182
WLM	75.9	-73.6	932 ± 33	-116
DDO210	34.0	-31.3	1071 ± 39	-137
M32	121.2	-22.0	785 ± 25	-205
IC10	119.0	-3.3	825 ± 50	-344
IC1613	129.8	-60.6	700 ± 35	-234
EGB0427+63	144.7	-10.5	1300 ± 700	-99

Table 1. All candidate members of the M31 sub-group initially considered in this study, along with positional information and heliocentric radial velocities. M32 is assumed to be at the same distance as M31. The three objects listed below M32 have had their distances and uncertainties taken from Mateo (1998); all those objects listed above M32 have had their distances and uncertainties taken from Papers I & II. The heliocentric radial velocities for all objects other than Andromeda IX are those listed by the NASA/IPAC Extragalactic Database (NED). Andromeda IX was only been recently discovered by Zucker et al. (2004) and its radial velocity has newly been measured by Chapman et al. (2005).

of the sky as M31 that are not located closer to the Milky Way than to M31. The majority of the distance estimates are taken from McConnachie et al. (2004c) (hereafter Paper I) and McConnachie et al. (2005) (hereafter Paper II) and will be discussed shortly. For those galaxies not analysed as part of our M31 survey (objects listed below M32 in Table 1), we take their distances from Mateo (1998). M32 is assumed to lie at the same distance as M31. The radial velocities for all objects other than Andromeda IX are those listed by the NASA/IPAC Extragalactic Database (NED). The radial velocity of Andromeda IX has been newly measured by Chapman et al. (2005) as part of the M31 radial velocity survey using the Deep Imaging Multi-Object Spectrograph on Keck II.

Table 2 lists the satellites of the Milky Way which will later be compared to the M31 satellites. The distance information is taken from Mateo (1998). Leo A is not considered a member of the Galactic satellite system due to its relatively large separation from the Milky Way. The putative dwarf galaxy in Canis Major (Martin et al. 2004) has not been included as its true nature is still the subject of some debate. The ultra-faint Galactic companion in Ursa Major (Willman et al. 2005) is not included as it has only recently been discovered and lacks a precise distance measurement.

Galaxy	l	b	r (kpc)
LMC	280.5	-32.9	49
SMC	302.8	-44.3	58
Sagittarius	6.0	-15.1	24 ± 2
Ursa Minor	105.0	+44.8	66 ± 3
Sculptor	287.5	-83.2	79 ± 4
Draco	86.4	+34.7	82 ± 6
Sextans	243.5	+42.3	86 ± 4
Carina	260.1	-22.2	101 ± 5
Fornax	237.1	-65.7	138 ± 8
LeoI	226.0	+49.1	250 ± 30
LeoII	220.2	+67.2	205 ± 12
Phoenix	272.2	-68.9	445 ± 30

Table 2. The satellites of the Milky Way and their Galactic coordinates. All distance information is taken from Mateo (1998).

2.2 M31-centric coordinates

It is convenient to use a M31-centric coordinate system for this investigation and we define a system that is directly analogous to Galactic coordinates, but centered on M31. In Galactic coordinates, the position of M31 is given by $(l_{M31}, b_{M31}, r_{M31})$. Another galaxy, S, has a position in Galactic coordinates of (l, b, r). The coordinates of S in a Cartesian coordinate system, centered on the Galaxy and aligned with l_{M31}, are

$$\begin{aligned} x &= r\cos(l - l_{M31})\cos b \\ y &= r\sin(l - l_{M31})\cos b \\ z &= r\sin b. \end{aligned} \quad (1)$$

The coordinates of S in the M31-centric spherical coordinate system are (l', b', r'), and are given by

$$\begin{aligned} l' &= \mathrm{atan}\left(\frac{y'}{x'}\right) + 180^\circ \\ b' &= \mathrm{asin}\left(\frac{z'}{x'}\right) \\ r' &= \left(x'^2 + y'^2 + z'^2\right)^{\frac{1}{2}} \end{aligned} \quad (2)$$

where

$$\begin{pmatrix} x' + r_{M31}\sin i \\ y' \\ z' + r_{M31}\cos i \end{pmatrix} = \mathbf{R}_y(90 - i)\,\mathbf{R}_x(90 - \theta)\,\mathbf{R}_y(-b_{M31}) \begin{pmatrix} x \\ y \\ z \end{pmatrix}. \quad (3)$$

We take $\theta = 39.^\circ8$ to be the position angle of the semi-major axis of M31 measured east from north in Galactic coordinates, and $i = 12.^\circ5$ as the inclination of M31 to the line-of-sight (de Vaucouleurs 1958). $\mathbf{R}$ is the appropriate Cartesian rotation matrix. The resulting coordinate system is directly analogous to the Galactic coordinate system but is centered on M31: l' is a longitude measured around the disk of M31, where $l' = 0$ is defined to be the longitude of the

Milky Way, and b' is a latitude, such that $b' = 0$ corresponds to the plane of the disk of M31. r' is the distance of S from the centre of M31. The Galaxy therefore lies at $(l' = 0, b' = -12.^\circ5, r' = 785\,\mathrm{kpc})$. Henceforth, the prime notation is dropped and the context will distinguish Galactic and M31-centric longitude, latitude and distance. The uncertainty in the distance to each candidate satellite translates into uncertainties shared by all three M31-centric coordinates, and whose relative sizes depend upon the location of the individual galaxy relative to M31.

2.3 Distance measurements

A study based on distances to multiple objects benefits from having small random errors associated with each measurement. It is then straightforward to account for the size of the error in the analysis procedure and assess the confidence of any results. However, for these methods to be reliable it is crucial that there are no systematic differences between the measurements which remain unaccounted for by the formal uncertainty.

Differential systematic uncertainties arise due to the heterogeneous datasets that are employed, the standard candle utilised, the observing/data reduction strategy and the algorithms applied to the data. Distances in astronomy are historically unreliable, even for the relatively nearby galaxies of the Local Group. It is important, therefore, to use a homogeneous set of distances which have differential systematic effects minimised. Any systematic uncertainties that may be present will then, presumably, affect each distance measurement in a similar way.

The I-band magnitude of the tip of the red giant branch (TRGB) is an observationally and theoretically well determined standard candle for relatively old, metal poor stellar populations. Using the Isaac Newton Telescope Wide Field Camera (INT WFC), we have obtained Johnson V and Gunn i photometry for a large number of Local Group galaxies, the majority of which are members of the M31 subgroup. In Paper I, we developed an analysis procedure to minimise the observational difficulties in measuring the location of the TRGB in a photometric dataset. Paper II then went on to apply this procedure to 17 Local Group galaxies for which we have INT WFC photometry and derived a homogeneous set of distances, as well as metallicities, for these objects. The identical data acquisition, reduction and analysis procedure for each galaxy goes a large way towards minimising differential systematic uncertainties, and the formal uncertainties on the measurements are $\sim 5\,\%$, similar to the Galactic satellites. The measurements are all consistent with previous estimates for each of the targeted systems, and there is no evidence for any systematic offsets or biases. The reader is referred to these papers for a more thorough discussion of these measurements. For the purposes of this study, there are a few systems that need to be considered for which we have not derived distances in this manner and it is necessary to supplement our data with that from other studies.

The distance to M31 is the key distance in this study. The distance calculated for it in Paper II is 785 ± 25 kpc. This measurement made use of stars in an annulus sampling the halo region of M31, minimising the influence of the young stellar populations and the substructure in this galaxy. The annulus was far enough from the centre of M31 so as not to be affected by crowding, significant extinction or serious contamination from disk and bulge components. Instead, it sampled a predominantly old, metal-poor population and the TRGB was obvious as an abrupt change in star counts in the luminosity function. Any line-of-sight effects through the halo would be expected to smear out the TRGB, which was not observed (if this effect was significant, then we would expect instead to have measured the TRGB for stars in the halo of M31 which are closer to us, and so the distance to M31 would be underestimated). The good agreement with recent RR Lyrae (794 ± 37 kpc; Brown et al. 2004), Cepheid (791 ± 40 kpc; Joshi et al. 2003) and independent TRGB distance measurements (783 ± 43 kpc; Durrell et al. 2001) suggests that our distance estimate is robust.

2.4 (In) completeness of the M31 subgroup

The pioneering survey by Sydney van den Bergh (van den Bergh 1972a,b) found the first dSph companions to M31: Andromeda I, II and III. This photographic (II-Iaj) survey was designed to detect objects fainter than the limits of the Palomar Sky Survey, and was extended in 1973 – 74 to encompass a total area of ~ 700 sq. degrees (van den Bergh 1974). No new dwarfs were discovered in this region. The limiting surface brightness to which this survey is complete is unknown, and the sky coverage becomes patchy beyond a projected distance from M31 of ~ 100 kpc. Subsequently, Armandroff et al. (1998, 1999) and Karachentsev & Karachentseva (1999) examined POSS II IIIaj survey plates in the vicinity of M31 and discovered three new companions to M31 (Andromeda V, VI, VII). During the same period, Whiting et al. (1997, 1999) conducted an all-sky search for new Local Group galaxies. While this search found two new Local Group galaxies, no new satellites of M31 were discovered.

The recent surveys for M31 satellites have been systematic in their sky coverage surrounding M31 and the discovery of bodies such as Andromeda V by Armandroff et al. (1998) (with a central surface brightness $\simeq$ 25.3 mags arcsec^{-2}; McConnachie & Irwin 2005b) show that they have been sensitive to low surface brightness features. It seems probable that all the dwarf galaxy companions to M31 with properties similar to those discovered prior to 2004 have been discovered, due to the large (~ 1500 sq. degrees), contiguous nature of the surveys. Some satellites, however, may lie directly behind the disk of M31. The area of sky covered by the disk of M31 behind which satellites could not be observed is $\sim 5 - 10$ sq. degrees; only one or two satellites are likely to hide from detection by this means.

The discovery of Andromeda IX, with a central surface brightness in V of 26.8 mags sq. arcsec^{-2} (Zucker et al. 2004) illustrates that the faint end of the M31 satellite luminosity function is yet to be fully explored. It is currently impossible to say if Andromeda IX is unique, or whether it is the first of many extremely low surface brightness M31 companions that await to be discovered. In the hierarchical CDM framework, the luminous satellites are expected to make up only a small subset of the total number of dark matter haloes (Kauffmann et al. 1993), with baryonic infall and star formation being suppressed in the majority, perhaps by reionisation or supernovae feedback (eg. Bullock et al. 2000;

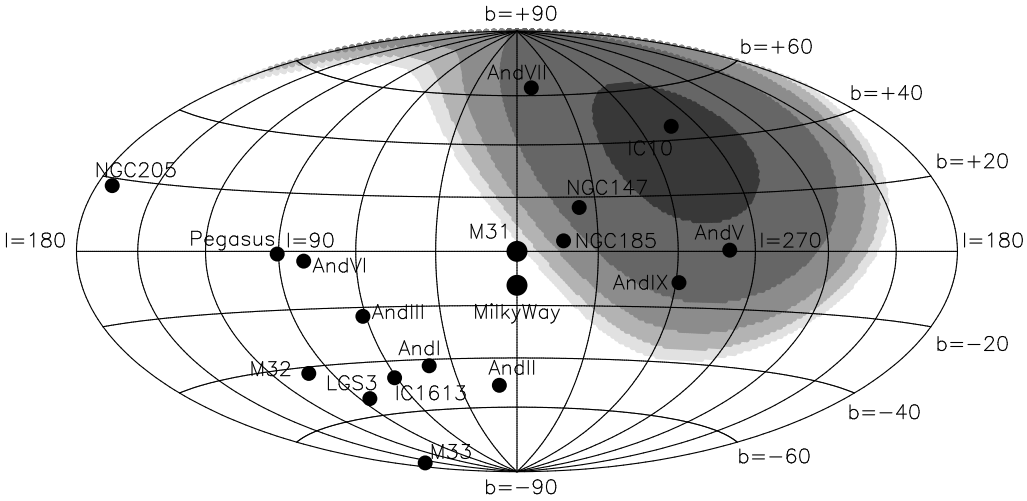

Figure 1. The influence of the Galactic disk on the detection of M31 satellites, as seen in the M31-centric coordinate system. Contours indicate the volume of space obscured by the Galactic disk. Objects residing in the region of sky indicated by the central contour will lie in the Galactic plane ($|b| < 15^\circ$ in Galactic coordinates) if they are ≥ 100 kpc from M31; objects lying inside the next contour will lie in the Galactic plane if they are ≥ 150 kpc from M31, and so on out to ≥ 300 kpc from M31 (outer contour). Shrinking of the contours by a factor of $2-3$ provides a good representation of the region of sky covered by the innermost $b = \pm 5^\circ$ of the Galactic disk, where we expect the extinction to be most extreme.

Dekel & Silk 1986). Cosmological simulations of galaxy formation have difficulty modelling all these processes, and star formation is usually dealt with by semi-empirical techniques. It is important to constrain the relative importance of these effects by obtaining an observational census of the number of these very faint luminous satellites around the Galaxy and M31. Several searches using SDSS are currently underway to do just this (Zucker et al. 2004; Willman et al. 2005). While these surveys are not yet completed, the results so far indicate that there is not a significant extra population of these objects.

To the north of M31 lies an area of sky obscured by the Galactic disk, which could hinder the detection of M31 satellites. Figure 1 shows an equal-area Aitoff projection of the satellites of M31 in the coordinates defined previously. Due to the orientation of M31 with respect to lines-of-sight through the Galactic disk, obscuration of M31 satellites is a function of position vector from M31. We consider the Galactic plane to defined by $|b| < 15^\circ$ in Galactic coordinates. Objects which reside in the region of sky indicated by the central contour will lie in the Galactic plane if they are ≥ 100 kpc from M31; objects lying inside the next contour will lie in the Galactic plane if they are ≥ 150 kpc from M31, and so on out to ≥ 300 kpc from M31 (outer contour).

Several galaxies reside in the most badly affected quadrant and a few of these, including one of the most intrinsically faint, lie in or near the Galactic plane in areas of significant extinction, namely And V, And VII, NGC 185, NGC 147 and IC10. For the first four of these galaxies, the level of extinction is modest, at $0.4 - 0.7$ mags in V. Only galaxies which were already intrinsically very faint (comparable to And IX) might be hidden by this level of extinction. On the other hand, IC10 is in a very heavily obscured region of the sky and, according to the extinction maps of Schlegel et al. (1998), has over 5 mags of extinction in V. The exact value is unreliable, given the patchy, irregular and large amount of extinction very close to the plane of the galaxy. If other M31 satellites lie in these heavily-obscured regions, it is not clear that they would have been easily observed; IC10 lends itself to discovery as it is currently undergoing a starburst. If the contours in Figure 1 are shrunk by a factor of 2 – 3, they provide a good representation of the area of sky covered by the innermost $b = \pm 5^\circ$ of the Galactic plane. This is the region of the Galactic plane where we are most likely to get these extreme reddening values. Considering the small area affected, it is unlikely that more than a few satellites (at most) will be affected.

3 MEMBERSHIP OF THE M31 SUBSYSTEM

A useful definition for the membership of the M31 satellite system are those objects whose kinetic energies are insufficient to escape the gravitational potential of M31. In addition, their separation must be small enough such that it is more likely for them to be bound to M31 rather than the Local Group as a whole. Choosing the correct membership is complicated by uncertainties in the mass and extent of the M31 halo, the separation of each candidate from M31 and the velocity of each candidate relative to M31. However, the uncertainty in the separation of the candidates from M31 is generally $\lesssim \pm 40$ kpc and is sufficient for this purpose. Likewise, the mass of M31, although not known precisely, is of order $1 - 2 \times 10^{12}\,M_\odot$ (Evans & Wilkinson 2000; Evans et al. 2000; Ibata et al. 2004; Fardal et al. 2005) and is sufficient to ascertain membership. The greatest practical uncertainty in determining membership of the M31 subgroup comes from the velocity estimate. Only the heliocentric radial velocity of M31 and its companions can be measured directly and from this an estimate needs to be made of their relative 3-dimensional velocity.

Einasto & Lynden-Bell (1982) demonstrated that the tangential velocity of M31 is small in comparison to the radial velocity under the assumption of no net angular mo-

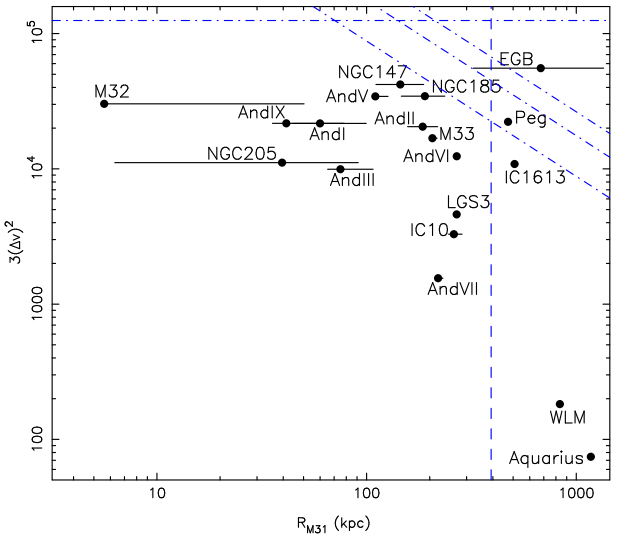

Figure 2. The distance of each candidate M31 satellite from M31 compared with an estimate of the potential required for the satellite to be virially bound to M31, as described in the text. Solid horizontal lines represent the uncertainty in the separation of each satellite from M31. The horizontal dot-dashed line represents the escape velocity from an isothermal M31 halo of circular velocity $\simeq 250\,\mathrm{km\,s^{-1}}$. The dotted lines correspond to the escape velocity for a point mass of $1, 2$ and $3 \times 10^{12}\,\mathrm{M}_{\odot}$. The vertical dashed line is the distance of M31 from the barycentre of the Local Group assuming the mass of M31 is of order the mass of the Galaxy. Galaxies lying in the area of the diagram that is approximately delimited by these lines are most likely satellites of M31.

mentum in the Local Group. Using this hypothesis, the total Galactocentric velocity of M31, $\mathbf{v}_{M31}$, is well approximated by the Galactocentric radial velocity component, $v_{r,M31} = -123\ \mathrm{km\,s^{-1}}$. We define the Galactocentric radial velocity of S, located at a position $\mathbf{r}_s$ from the Galactic centre, to be $v_{r,s}$. The component of the velocity of S with respect to M31 in the direction $\hat{\mathbf{r}}_s$ is then

$$\Delta v = v_{r,s} - v_{M31}\hat{\mathbf{r}}_s.\hat{\mathbf{r}}_{M31}\ , \qquad (4)$$

where $\hat{\mathbf{r}}_s$, $\hat{\mathbf{r}}_{M31}$ are unit vectors. Independent velocity information for S in the remaining two orthogonal directions is unavailable. We therefore assume equipartition of kinetic energy and multiply $(\Delta v)^2$ by a factor of three. The resulting quantity is an estimate of twice the specific kinetic energy of the galaxy, corresponding to an estimate of the gravitational potential required for the putative satellite to be virially bound to M31. In Figure 2, we plot this quantity against the separation from M31 for each candidate satellite. The horizontal solid lines indicate the uncertainty in the separation of each candidate from M31. The horizontal dashed line corresponds to the escape velocity from an isothermal halo with a circular velocity of $\simeq 250\ \mathrm{km\,s^{-1}}$. The dotted lines correspond to the escape velocity for a point mass of $1, 2$ and $3 \times 10^{12}\,\mathrm{M}_{\odot}$. While these mass profiles are unrealistic, they represent simple models which bracket the extremes of the global potential, without being too prescriptive. The vertical line is the distance of M31 from the barycentre of the Local Group, assuming that the masses of the Galaxy and M31 are roughly equivalent. Objects lying in the area defined by these lines are probably satellites of M31.

Figure 2 shows that M32, NGC 205, 147, 185, Andromeda I, II, III, V, VI, VII and IX, LGS3, IC10 and M33 are likely bound satellites of M31. The membership of Pegasus and IC1613 to the M31 subgroup is marginal as they are located $\sim 500\,\mathrm{kpc}$ from M31. Nevertheless, we consider them to be members as their current position relative to M31 and the Galaxy means that their orbits are almost certainly dominated by the potential of M31. WLM and Aquarius are located $\sim 1\,\mathrm{Mpc}$ from M31, and should not be considered as satellites. The separation and velocity of EGB0427+63 means that it, too, is unlikely to be a satellite.

4 THE 3D DISTRIBUTION OF THE ANDROMEDA SUBGROUP

Figure 3 shows the 3-dimensional distribution of the 16 members of the M31 subgroup. The plane indicated is aligned with the disk of M31 and each grid cell is $100 \times 100\,\mathrm{kpc}$. Solid lines are used for satellites that lie above the plane of the disk and dotted lines are used for satellites that lie below the plane of the disk. The direction of the Galaxy is marked. The top panel of Figure 4 shows the same distribution as an equal-area Aitoff projection of the M31-centric l and b coordinates. The position of the Galaxy is included as a reference. The lower panel shows error bars which represent the combined uncertainty in the position of each satellite due to the uncertainty in its distance and in the distance to M31. The positions of M32, NGC 205 and Andromeda IX in this projection are sensitive to these uncertainties due to their close proximity to M31, but the positions of the majority of the satellites are relatively well constrained.

Several general points are clear from inspection of the top panel of Figure 4. For example, half of the satellites lie within $|b| \lesssim 20^{\circ}$ of the disk of M31. The satellite distribution as a whole does not appear isotropic; the upper left quadrant and lower right quadrant house only one satellite each, while the remaining fourteen are confined to the other two quadrants. In addition, the satellites appear to congregate within 90° of $l = 0$.

4.1 Variation with latitude

In the lower panel of Figure 5, the differential absolute (M31-centric) latitude distribution of the M31 satellites is plotted. In the top panel, we show the Galactic satellite distribution as a comparison (in Galactic coordinates). The putative dwarf galaxy in Canis Major (Martin et al. 2004) has been highlighted in the upper panel as a dot-dashed line. The dashed curves correspond to an isotropic distribution of satellites. The correct null hypothesis for a CDM distribution of satellites may not be isotropy, however, as the satellites are expected to have a prolate distribution (Zentner et al. 2005). This makes no difference to the following discussion.

With the inescapable caveat of small-number statistics, the M31 satellite distribution is qualitatively similar to the isotropic distribution and suggests that isotropy is a reasonable first-order assumption for the latitude distribution of satellites. Formally, a Kolmogorov-Smirnov (K-S) test between the Galactic and M31 distributions shows that the two populations are not significantly statistically different.

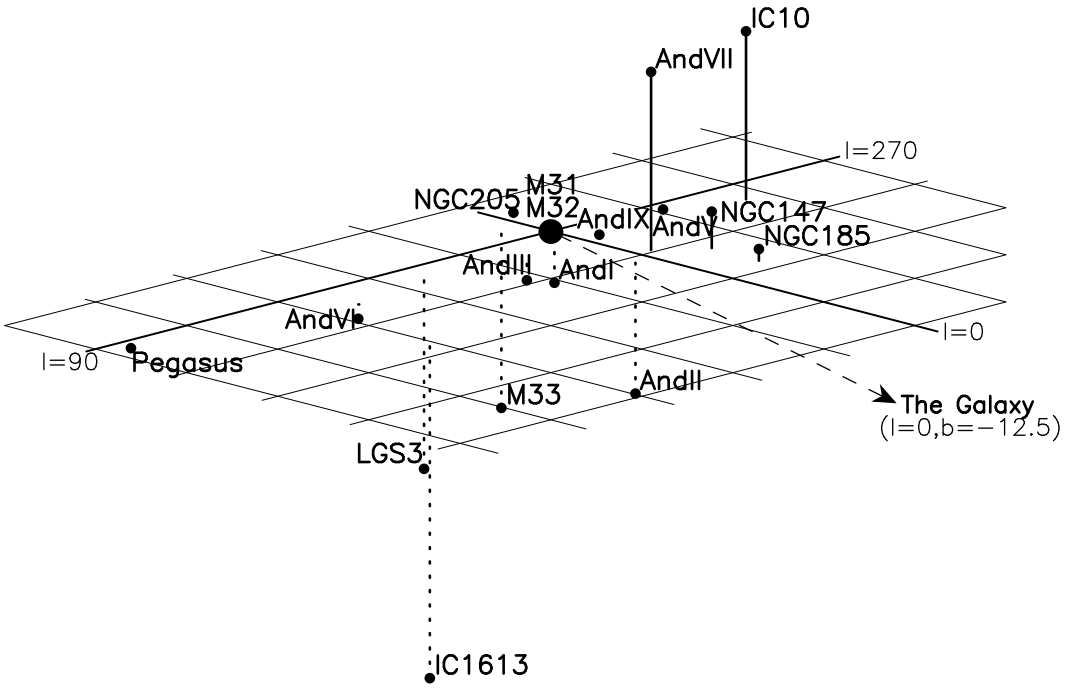

Figure 3. A three-dimensional representation of the spatial distribution of the M31 subgroup. The plane shown is aligned with the disk of M31. Each grid cell is 100×100 kpc. l and b are the M31-centric spherical coordinates defined earlier. Solid lines are used for satellites lying above the disk, while dotted lines are used for satellites lying below the disk. The direction of the Galaxy is marked.

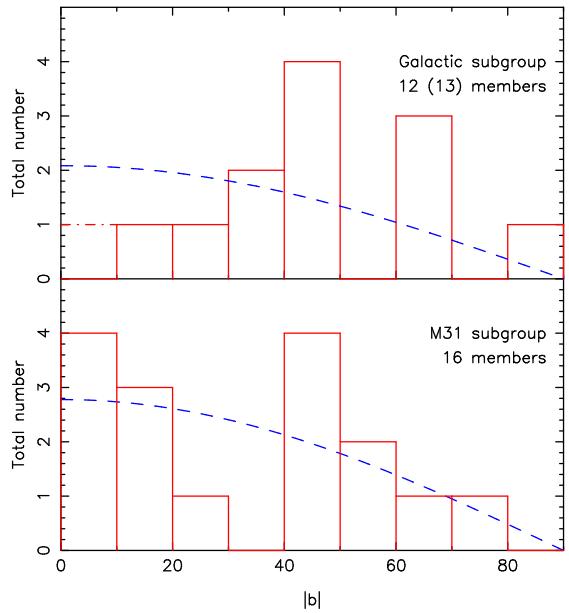

Figure 5. The differential absolute latitude distribution of the Galactic (upper panel) and M31 (lower panel) subgroups. The dashed curves shows an isotropic distribution for the same total number of satellites. Also shown as a dot-dashed line in the top panel is the position of the putative Galactic satellite in Canis Major. There is an apparent deficit of Galactic satellites at low latitudes, which is most readily explained as a selection effect due to obscuration by the Galactic disk. The M31 and Galactic latitude distributions are not statistically different however; a K-S test shows they are consistent with being drawn from the same underlying distribution at the 38 % level.

They are consistent with being drawn from the same underlying distribution at the 38 % level. The inclusion of Canis Major makes the distributions consistent at > 60 % probability. However, the Galactic system has an apparent underabundance of satellites at low latitudes in comparison to the isotropic case and to M31; only one (definite) satellite is observed around the Galaxy at $|b| < 20^\circ$ (Sagittarius) compared to seven around M31. If the Galactic satellites follow an isotropic distribution, then we would expect ~ 4 satellites to be located at $|b| < 20^\circ$, instead of the 1(2) so far discovered. This implies that obscuration by the Galactic disk at low Galactic latitudes may have led to an incompleteness in the Galactic subgroup of $15 - 25$ %. While approximate, these values agree with the study by Willman et al. (2004), who conclude that there may be a ~ 33 % incompleteness in the Galactic satellites caused by obscuration at low latitudes.

4.2 Radial distribution

The top panels of Figure 6 show the differential radial distribution of Galactic satellites (left) and M31 satellites (right). The lower panels show the respective cumulative distributions. The abscissa have not been normalised by the virial radii of the host haloes because these are uncertain and are believed to be similar for the two hosts (258 kpc for the Galaxy, 280 kpc for M31; Klypin et al. 2002). The Galactic subgroup is noticeably more centrally concentrated than the M31 subgroup; half of the Galactic satellites are within ~ 100 kpc while the corresponding separation for the M31 system is ~ 200 kpc. However, the distributions are not statistically different; a K-S test on the distributions, normalised to the same total number of satellites, shows there is

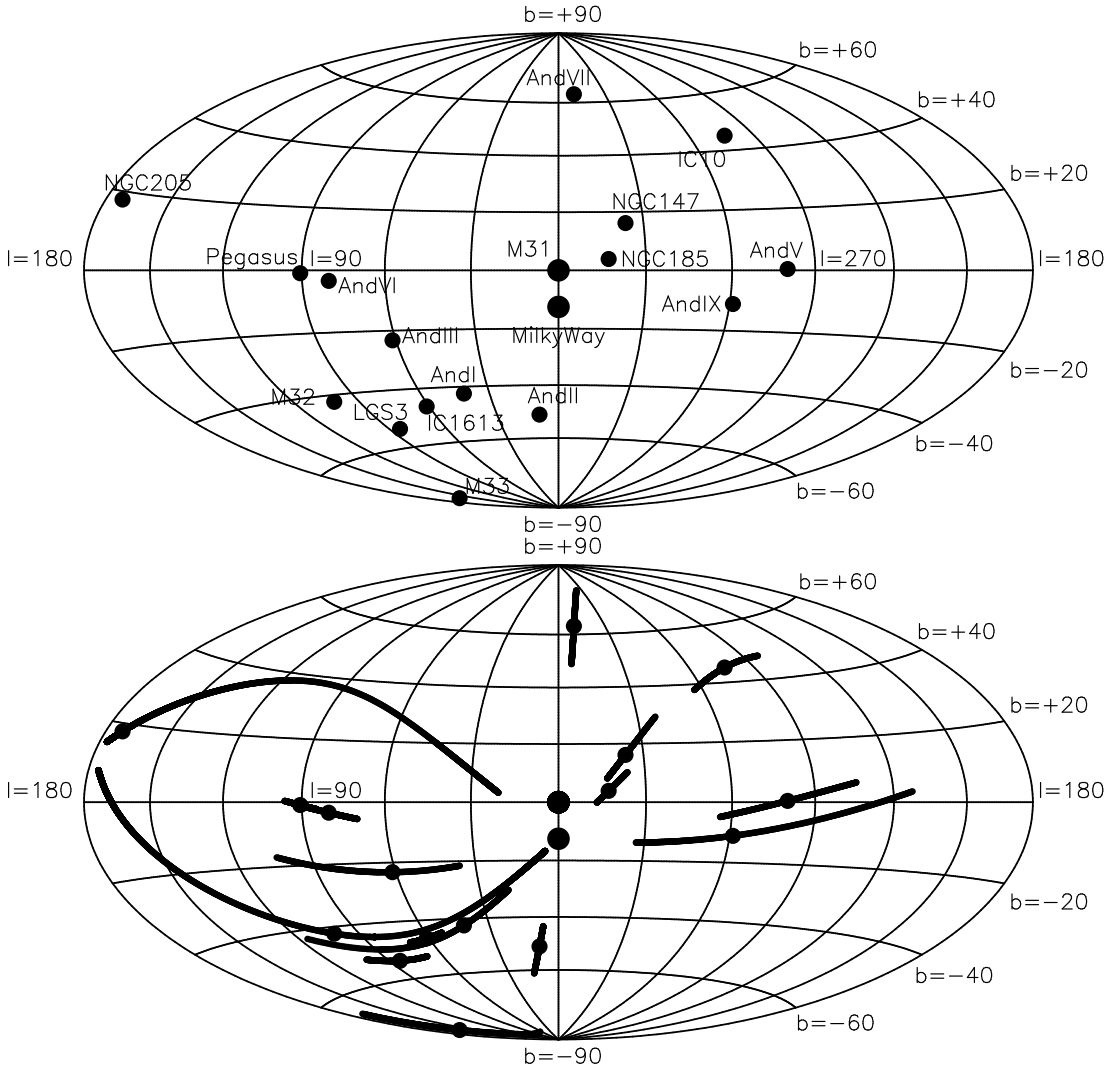

Figure 4. Top panel: An Aitoff equal-area projection of the M31 satellite distribution, in the M31-centric spherical coordinates defined earlier. The position of the Galaxy is shown for reference and is defined to lie at $l = 0$. Bottom panel: Same as top, but now with error bars showing the combined uncertainty in the position of each satellite, due to the uncertainty in its distance and in the distance to M31. The positions of NGC 205, M32 and Andromeda IX are relatively uncertain due to the close proximity of these objects to M31. All of the other satellites occupy relatively well-defined positions.

a 24 % chance that they are drawn from the same underlying distribution.

In a recent study, Willman et al. (2004) compared a simulated CDM radial distribution of satellites with those for the Galaxy and M31. These distributions were compared by assuming that dwarfs inhabit the sub-haloes with the highest circular velocity at zero redshift, and assuming that the Galactic satellite system is incomplete beyond 100 kpc. Based upon this comparison, they concluded that the Galactic system is potentially incomplete by a factor of up to 3 (including the effects of incompleteness at low Galactic latitude), and that there may be some satellites beyond 100 kpc which have eluded detection, with absolute magnitudes and central surface brightnesses similar to the detected population.

As the discovery of the ultra-faint stellar system in Ursa Major illustrates (Willman et al. 2005), it is almost certainly the case that very faint satellites still await to be discovered around the Galaxy. It is also likely that the Galactic disk hinders the detection of low latitude Galactic satellites. It is not so clear, however, that there is significant incompleteness in the outer (> 100 kpc) halo. Irwin (1994) conducted an automated search of Schmidt sky survey plates for Galactic satellites, covering $\sim 2/3$ of the sky and extending down to a Galactic latitude of $|b| = 20^\circ$. This survey was sensitive enough to detect systems such as Draco and Ursa Minor out to 300 kpc. Only Sextans was found (Irwin et al. 1990). The survey could have found systems up to one magnitude fainter than Sextans out to a distance of 200 kpc. Despite analysing more than 1000 sky survey plates, covering both hemispheres, no other comparable satellites were found. In addition, given that the total numbers of satellites around M31 and the Galaxy are roughly equivalent, and that by normalising the populations by total number the distributions are broadly similar, it seems unlikely that the Galactic

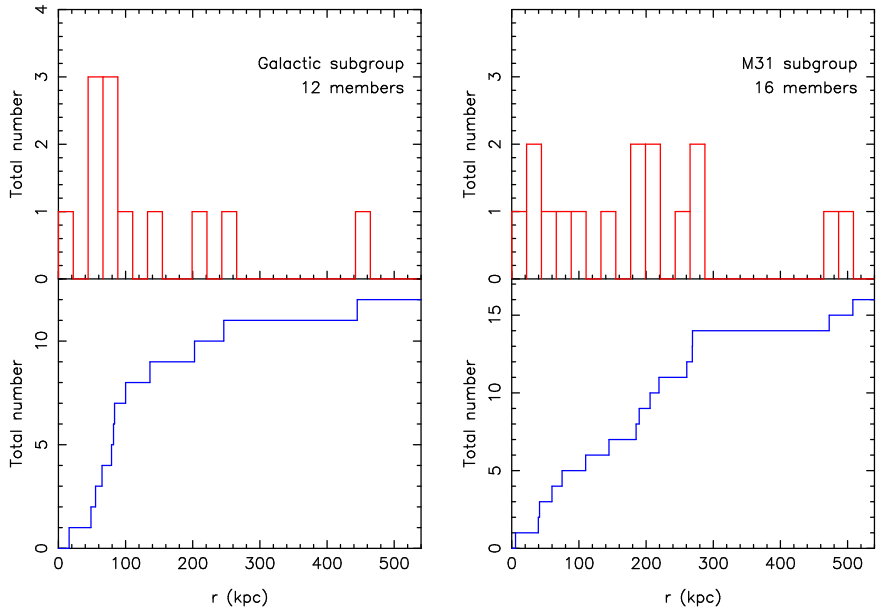

Figure 6. The differential radial distribution of Galactic satellites (top left) and M31 satellites (top right). The lower panels show the respective cumulative distributions. The Galactic subgroup is more centrally concentrated than M31; roughly half of its members are located within 100 kpc compared to ~ 200 kpc for M31. A K-S test, where the populations are normalised to the same total number of satellites, shows the distributions are not significantly statistically different; formally, there is a 24 % chance that they are drawn from the same underlying distribution.

population is seriously incomplete in the manner suggested by Willman et al. (2004).

4.3 Distribution with respect to the Galaxy

Figure 7 is the Aitoff projection shown in Figure 4 with a dashed line representing the plane separating the near side of M31 from the far side, with respect to the Galaxy. Objects lying inside this line lie on the near side of M31, while objects lying outside this line lie on the far side of M31. Neglecting distance uncertainties, NGC205 is the only object that clearly lies on the far side of M31; the other satellites are all close to, or in front of, the plane. It is important to emphasise that this plane is not a fit, and is defined only by the position of the Galaxy with respect to M31. In fact, fourteen satellites lie in front of the plane and two behind it. A suitable null hypothesis is that a satellite is equally likely to lie in front or behind this plane. This is easily tested with binomial statistics and is inconsistent with the observed distribution at 99.8 %. This does not take into account the distance uncertainty associated with each satellite. Therefore, we have also adopted a Monte-Carlo sampling technique where we continually generate new M31 satellite distributions by choosing the distance of M31 and its satellites from Gaussian distributions centered on the distance given for them in Table 1, with a standard deviation equal to the corresponding distance uncertainty. Only in 0.5 % of the generated cases do we find a distribution with equal numbers of satellites in both hemispheres, indicating that the anisotropy is not an artifact of the distance uncertainties.

Figure 8 shows the positions of the satellites in a Cartesian coordinate system, such that the abscissa is aligned with the line-of-sight to M31. $(x_{M31} = 0, y_{M31} = 0, z_{M31} = 0)$ is the position of M31 and $(x_{M31} = 785, y_{M31} = 0, z_{M31} = 0)$ is the position of the Galaxy. The distribution in the top-panel is affected most by the distance uncertainties, and the dot-dashed line represents the corresponding histogram for the Monte-Carlo distributions generated previously.

For an isotropic distribution of satellites, the geometric centre of the satellite distribution is expected to be coincident with the position of the host. It is straightforward to calculate the mean (or median) and random error in the mean ($\sigma = \sigma_d/\sqrt{N}$, where σ_d is the standard deviation) for the three distributions shown in Figure 8. The random error in the mean is the relevant statistic to use in this case, as individual uncertainties in the position of each data-point statistically average out when looking at the distribution of all data points (assuming these uncertainties are of comparable magnitude and are random). As the distributions deviate from Gaussians, we have calculated σ_d using the more robust median-of-the-absolute-deviation-from-the-median (MAD) statistic (Hoaglin et al. 1983). This is given by

$$MAD = median\,|x_i - median\,(x)| \qquad (5)$$

and is related to σ_d by $\sigma_d = 1.48 \times MAD$ for a Gaussian. This statistic gives an estimate of the scatter in a distribution even if it deviates significantly from a Gaussian and contains several outliers. We have also calculated σ_d using the mean-of-the-absolute-deviation-from-the-mean statistic, finding good agreement with the MAD statistic.

The mean, median and σ for all the M31 satellites are listed in Table 3. Also listed are the equivalent numbers when the outlying satellites Pegasus and IC1613 are excluded. Table 4 lists the equivalent results for the Galactic satellite system, where the coordinate system has been shifted to be centered on the Galaxy. For this system, the

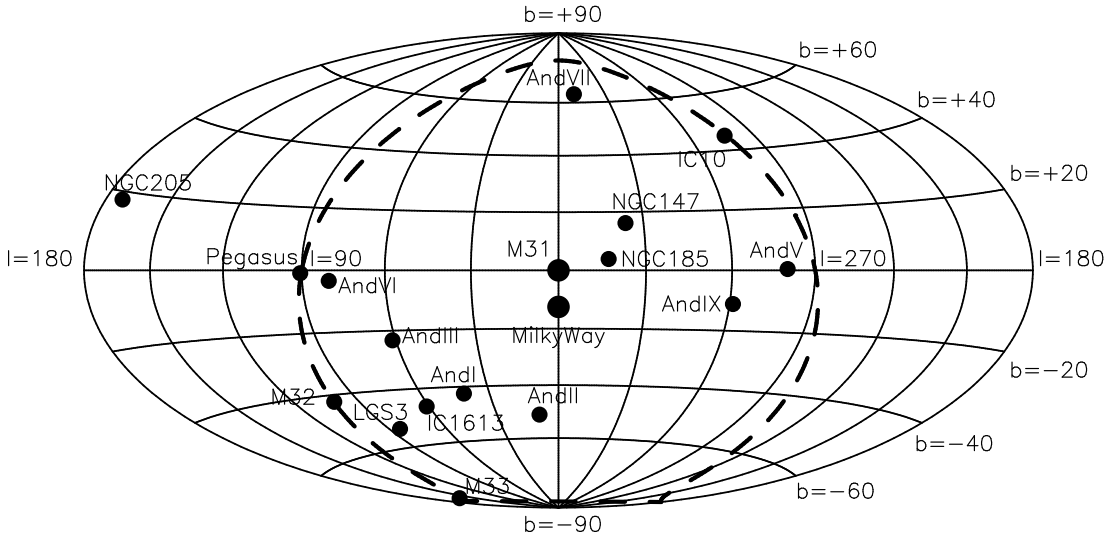

Figure 7. Same as Figure 4, but with a dashed line indicating the plane which separates the near side from the far side of M31. The satellites of M31 show a correlation with this plane, such that they preferentially lie on the near side of M31 with respect to the Galaxy.

	All satellites			Excluding Peg + IC1613		
(kpc)	mean	median	$\sigma = \sigma_d/\sqrt{N}$	mean	median	$\sigma = \sigma_d/\sqrt{N}$
x_{M31}:	58	40	14	49	40	12
y_{M31}:	-55	-10	21	-7	-5	19
z_{M31}:	-25	-5	16	-5	-4	17

Table 3. The mean, median, and random error in the mean (σ) for the three distributions shown in Figure 8. These have been calculated for the case where all the satellites are included and for the case where the outlying Pegasus and IC1613 dwarfs are excluded.

random error on the mean is of a similar magnitude, or greater, than the mean/median of each coordinate. This suggests that there is no statistically significant offset between the centre of the Galactic satellite system and the Galaxy. Likewise, for the M31 subgroup, there is no statistically significant offset between the centre of its satellite system and M31 for y_{M31} and z_{M31} (taking into account the effects of the two outliers). However, the mean/median of x_{M31} is inconsistent with zero at the $3\,\sigma$ level. This suggests that the satellite distribution of M31 is significantly offset from M31 in the direction of the Galaxy/barycentre of the Local Group at the $3\,\sigma$ level.

It is pertinent to calculate whether an equivalent asymmetry exists in the velocities of the satellites. Using the notation defined in Section 3, the mean velocity of the satellites relative to M31 in the direction of the Galaxy is estimated as $\langle \Delta\, v \rangle \,/\, \langle \cos\theta_{M31} \rangle$, where $\cos\theta_{M31} = \hat{\mathbf{r}}_s.\hat{\mathbf{r}}_{M31}$. This is the projection of the relative velocity of the satellite with respect to M31 onto the line-of-sight to M31, and is $+19\pm21\,\mathrm{km\,s^{-1}}$. A positive sign indicates that the satellites are approaching more slowly than M31. The uncertainty is the random error in the mean, and the velocity offset is not statistically significant.

5 GHOSTLY STREAMS?

Using the 3-dimensional information available on the M31 satellite distribution it is possible to search for "ghostly streams" of satellites around M31 in a similar way to Lynden-Bell & Lynden-Bell (1995). This requires finding satellites that align on great circles, which may reflect a stream-like origin and assumes that there has not been significant precession of the orbits which would wash out any alignments, as would be expected if the halo of M31 is flattened. Here, we assume this is not the case.

The probability of finding n satellites from a sample of N in one particular plane is readily estimated from binomial statistics and is small if n is a large fraction of N. However, the probability of finding n satellites in any plane is much larger and reflects the fact that all possible planes will have been tried in the search for the plane around which the scatter is smallest. This point is relevant to the claim by Kroupa et al. (2005) that the planar distribution of Galactic satellites is inconsistent with being drawn from a spherical distribution. This is only true at a high significance level if the plane in which the satellites align is considered to be predefined.

Figure 9 is a Lambert equal-area zenithal projection of the polar paths of the satellites of M31. Each curve corresponds to the track containing all points in the northern hemisphere perpendicular to the vector connecting the satellite to M31. Where each curve crosses another defines the pole of the plane containing the two satellites and M31, and is equivalent to the direction obtained on taking the cross-product of the position vector of the satellites from M31. Points at which multiple paths cross define the poles of planes which contain candidate streams of satellites.

Several possible streams are highlighted by Figure 9 but

(kpc)	mean	median	$\sigma = \sigma_d/\sqrt{N}$
$x_{M31} - 785$:	19	15	16
y_{M31}:	3	-14	20
z_{M31}:	-43	-26	21

Table 4. The same statistics as in Table 3 but for the Galactic satellite system. The coordinates are the same as defined previously, but shifted to be centered on the Galaxy instead of M31. No statistically significant offsets are observed between the satellite distribution and the Galaxy.

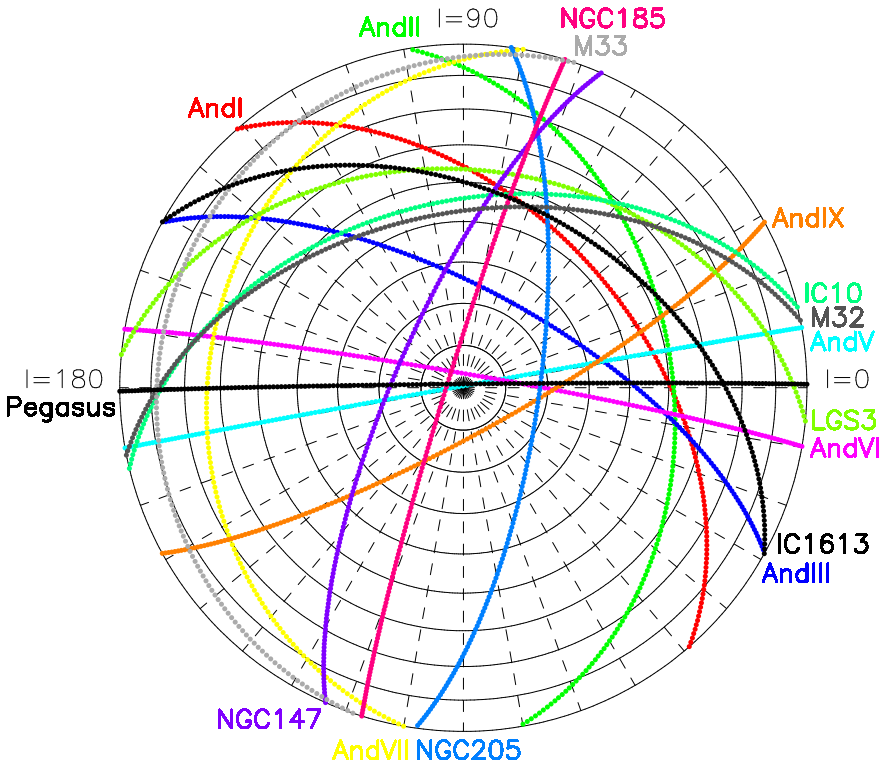

Figure 9. A Lambert zenithal equal-area projection. l increases anticlockwise as shown. b decreases radially from $b = 90°$ at the centre to $b = 0$ at the perimeter; the embedded circles represent 10° increments in b. Each curve represents the northern 'polar path' of the labelled M31 satellite ie. the track representing all points tangential to its direction from M31. The point at which two tracks cross defines the pole of the plane containing the two objects and M31. Points at which multiple tracks cross define the poles of possible streams containing the relevant satellites and M31.

attributing significance to them without kinematic information is premature. For example, the projected position of M32 is sufficiently unreliable to neglect it in this analysis, and NGC 147 and 185 are probably a binary system (van den Bergh 1998), so should really be treated as a single point.

However, there are numerous possible candidate streams indicated in Figure 9, of which some of the most well defined are:

- M33, Pegasus, IC10 (and possibly M32) ($l \simeq 180°, b \simeq 12°$);
- Andromeda III, VII and LGS3 ($l \simeq 140°, b \simeq 23°$);
- NGC 185, 147 and 205 (and possibly Andromeda II ($l \simeq 74°, b \simeq 24°$);
- Andromeda I, IC10, 1613, NGC147 and 185 (and possibly M32) ($l \simeq 80°, b \simeq 42°$);
- Andromeda II, IC10 and LGS3 (and possibly M32) ($l \simeq 50°, b \simeq 30°$);
- Andromeda III, V and IX ($l \simeq 10°, b \simeq 56°$);
- Andromeda V, VI and Pegasus ($l \simeq 0, b \simeq 80°$). Andromeda IX and NGC 205 share a pole nearby at ($l \simeq 0, b \simeq 72°$);
- Andromeda I, II, III, and VI ($l \simeq 352°, b \simeq 38°$)

Without doubt many, if not all, of these associations are chance alignments; it is difficult to think of a plausible physical association between M33, Pegasus, IC10 and M32, for example. However, a few streams could be viable, such as those defined by the dwarf ellipticals or some of the dwarf spheroidals. It is particularly interesting to note the planes defined by the latter group; Andromeda I, II, III, V, VI and IX all share poles in the same general vicinity of ($l \sim 0, b \sim 60°$) and the great circle that they loosely form is readily identified in Figure 4. These constitute six of the

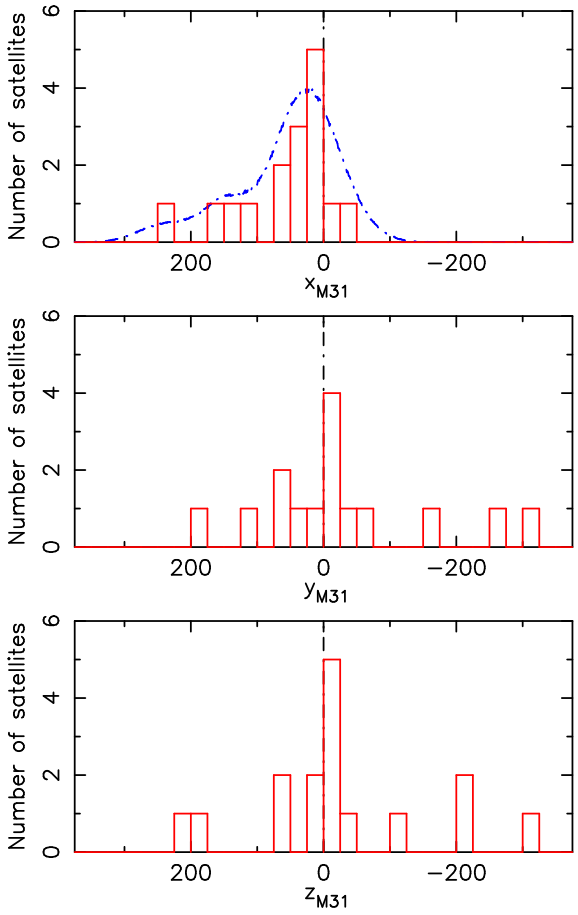

Figure 8. Distribution of satellites along the line-of-sight to M31 (top panel) where $(x_{M31} = 0, y_{M31} = 0, z_{M31} = 0)$ is the position of M31 (dot-dashed vertical line) and $(x_{M31} = 785, y_{M31} = 0, z_{M31} = 0)$ is the position of the Galaxy. The satellite distributions in the two directions orthogonal to this (middle and bottom panels) are also shown. Distance uncertainties mostly affect the distribution in x_{M31}. To illustrate this, the blue dot-dashed curve shows the distribution of satellites along the line-of-sight to M31, derived by continually drawing the distance of M31 and its satellites from Gaussian distributions centered on their derived distance with a standard deviation equal to their distance uncertainty.

seven dSph companions to M31 and have broadly similar star formation histories and colours (Paper II). A physical association between some or all of these objects may therefore be plausible, and could represent analogous systems to the Magellanic or FLS streams proposed around the Galaxy.

Further analysis of the planes listed above requires an investigation of the kinematics of the candidate streams. The study of the Galactic satellites by Lynden-Bell & Lynden-Bell (1995) investigated the specific energy of the members of the proposed streams, under the assumption that they were physically associated with each other and had the same specific angular momentum, invariant with time. The derived specific energies of the putative members are then expected to be equal if the satellites are physically associated. The specific energy of each satellite is given by

$$E = \frac{1}{2}v_G^2 + \frac{1}{2}h^2 r^{-2} - \phi \ , \qquad (6)$$

where v_G is the Galactocentric radial velocity of the satellite, h is the specific angular momentum and ϕ is the gravitational potential of the Galaxy at the location of the satellite. The first term represents the energy due to the radial motion of the satellite; the second term is the rotational kinetic energy of the satellite in its orbit, where h has been assumed to be a common constant for all stream members.

An equivalent kinematic analysis to that of Lynden-Bell & Lynden-Bell (1995) is not directly possible for the M31 satellites. The heliocentric radial velocities that are measured for these objects do not provide full information on the M31-equivalent of v_G and therefore the first term of Equation 6 cannot be calculated. This will remain the case until proper motions for the M31 satellites become available. The additional uncertainties on the correct form and magnitude of ϕ, the distance uncertainties and the unknown contribution of interlopers to the make-up of the candidate streams (which may be as high as 100 %) also makes a numerical approach to this problem unsatisfactory without prior information on the orbits of at least some of the satellites. Without this information, any conclusions on the physical association, or otherwise, of the members of the M31 subgroup are likely to be highly vulnerable and uncertain.

6 INTERPRETATION

Using the distances derived in Papers I and II, we have found that the M31 satellites are distributed anisotropically along the line-of-sight to this galaxy, and are skewed such that most satellites are on the near-side of M31. We have quantified this distribution and measure a ≥ 40 kpc offset between the centre of the M31 satellite system and M31. This offset is in the direction of the Galaxy/Local Group barycentre, and is significant at the $3\,\sigma$ level.

We have also examined the spatial distribution of the M31 subgroup using earlier distance estimates to M31 and its satellites tabulated in Mateo (1998) (Andromeda V, VI, VII and IX are recent discoveries and are not included in this paper, so we kept their distances the same). The larger distance errors in most of the other measurements and the inhomogeneous nature of the distance estimates which make up this compilation, unsurprisingly dilute, although do not remove, the asymmetry observed in the distribution.

One of the primary motives of this paper was to make use of more accurate and more consistent distance estimates to study the satellite distribution of the M31 system. These estimates are the key to the subsequent analyses (see Section 2.3) and a comparison of them with respect to previous distance estimates is given in Paper II. The significant benefit obtained by using this dataset is that all of the measurements are obtained on the same system and in this respect represent the most homogeneous Local Group distance estimates available. The distance estimate to M31 is clearly the most critical and bringing M31 closer by 25 – 60 kpc would remove the anisotropy. While this is a possibility, it requires the TRGB measurement to M31 to be systematically offset relative to the other TRGB measurements. The TRGB analysis, however, was designed to min-

imise the probability of this occurring. The possible errors which could affect M31 in particular were discussed in detail earlier. In addition, this interpretation would require other TRGB (Durrell et al. 2001), RR Lyrae (Brown et al. 2004) and Cepheid (Joshi et al. 2003) distances to M31 to be wrong in similar ways by similar amounts. If M31 is located at $\sim 740\,\mathrm{kpc}$, it is not obvious why all the recent distance estimates to it, which have made use of a range of independent standard candles, should produce very similar wrong answers. As such, we believe that this is the most unlikely interpretation of the result. It should not be neglected, but it potentially has much wider reaching consequences for the use of these distance indicators.

Selection effects were discussed in Section 2.4. It is hard to understand how this result could be explained by this means. We are unaware of any effect which would prevent the detection of M31 satellites located between $800 - 1000\,\mathrm{kpc}$ from the Galaxy, assuming that they plausibly have typical properties of the satellite system. These satellites would have to be located directly behind the disk of M31 to evade detection, and this is a very specific and small volume of space. Only $\sim 5 - 10\,\mathrm{sq.\,degrees}$ of sky are masked by M31, compared to the $\sim 1500\,\mathrm{sq.\,degrees}$ over which satellites have been surveyed for and discovered.

It is an interesting question to ask if such an offset could have a dynamical origin. The main difficulty with a dynamical solution is timescale: the orbital (dynamical) timescale of a satellite at a distance of $\sim 100-200\,\mathrm{kpc}$ from a $\sim 10^{12}\,M_{\odot}$ host is 1.6 – 4.5 Gyrs, meaning that satellites will have completed > 3 orbits around M31 over the course of a Hubble time. Given this, it is unlikely that any anisotropy present in the satellite distribution could survive over a Hubble time, and suggests that it was either introduced recently or maintained somehow. Further, any dynamical effect is presumably going to affect both the luminous satellites and the dark matter satellites, and so we would assume that the dark matter satellites must also be asymmetrically distributed in this manner.

A scenario in which a satellite spends a larger fraction of its orbital period on the near side of M31 than the far side is easily envisaged in a simple point mass case. Here, if the major axis of the orbit of the satellite is aligned with the position vector of the Galaxy, and M31 is at the far focus of the elliptical orbit, then the satellite is more likely to be observed on the near side of M31, as given by Kepler's laws. In reality, the potential of M31 is not that of a point mass and there is the added complication that the orbits of the satellites need to be correlated. If the M31 subsystem consists of dynamical groupings of satellites (Figure 9), then the probability of observing a heavily-skewed distribution might be expected to increase, as there are fewer independent satellite orbits. However, orbital precession in a non-spherical halo potential would destroy any initial correlations present. This may either indicate that many of the dwarf satellites of M31 were accreted relatively recently (within the past dynamical time or so) or that the outer potential of M31 is approximately spherical. There is a growing body of evidence from simulations of galaxy formation that the observed dwarfs consist of objects which were accreted relatively recently (eg. Bullock & Johnston 2004; Abadi et al. 2005), else it is unlikely they could have survived tidal disruption until the present. This may help explain the skewed distribution.

Another possible dynamical explanation could be that the M31 satellite galaxies are tracing the large-scale structure of the nearby Universe. According to CDM structure formation, satellite galaxies are accreted preferentially along filaments. It may be, therefore, that the satellites were accreted along a filament that aligns with the Galaxy/Local Group barycentre, or that the satellites are tracing a dark filament that aligns with this direction. Alternatively, the potential around M31 may be asymmetric due to contributions from other Local Group components e.g. a large Local Group halo and/or a contribution from the halo of the Galaxy, if it is significantly extended. This latter scenario will have been particularly relevant at early times when the separation of the M31 – Galaxy binary system was much less (the timing argument: Kahn & Woltjer 1959; Lynden-Bell 1981) and if the Galaxy is significantly more massive than M31. However, effects such as precession could once again act to destroy any gross asymmetries present.

van den Bosch et al. (2005) have recently shown from an analysis of the Two-Degree Field Galaxy Redshift Survey (2dFGRS) that, in general, the brightest galaxy in a group is offset in velocity from its satellites, and has a specific kinetic energy that is $\sim 25\,\%$ of its satellites. For a relaxed CDM halo, this corresponds to an offset of the brightest galaxy from its satellite system of $\sim 3\,\%$ of its virial radius, or of order 10 kpc for M31. The associated velocity offset is a few tens of $\mathrm{km\,s^{-1}}$. They suggest that the brightest galaxy either oscillates around the minimum of the relaxed halo potential (which is unlikely if the system has a cusp rather than a core), or that it resides at the minimum of the halo potential which is not yet relaxed.

It is unclear whether the scenarios developed by van den Bosch et al. (2005) could apply to M31. These authors analysed groups of galaxies defined by four or more members in the 2dFGRS picked out using a group-finding algorithm developed by Yang et al. (2005). The redshift range of these systems is $0.01 \leq z \leq 0.2$. They found that for systems where the velocity dispersion was less than $200\,\mathrm{km\,s^{-1}}$ (corresponding to a total mass of $< 10^{13}\,M_{\odot}$), the central galaxy was consistent with being located at rest at the centre of the group. However, for this mass range, it was also consistent with being marginally displaced from the centre. It may be, therefore, that the anisotropic satellite distribution of M31 is tentative evidence that the halo of M31 is not yet relaxed. To the best of our knowledge, there is currently no study which gives the virialisation timescale of halos formed in a CDM hierarchy as a function of mass. The rather unusual distribution of satellites of M31 that we have discovered surely merits further theoretical studies.

7 SUMMARY

We have re-derived membership of the M31 subgroup by examination of the positions and kinematics of the putative members, and discussed their distance estimates and completeness. Using an M31-centric coordinate system, we have compared the distribution of satellites above and below the disks of M31 and the Galaxy. This suggests that the Galactic system is incomplete at low latitudes by $\sim 20\,\%$. Likewise, comparison of the radial distribution of satellites around these two hosts show that the M31 system is less cen-

trally concentrated than the Galactic system. We have also searched for "ghostly streams" of satellites around M31, in a similar way as Lynden-Bell & Lynden-Bell (1995) did for the Galactic system, and find several, including some which contain several of the dwarf spheroidal companions. Unfortunately, the current lack of proper motion data for these objects does not allow the possible physical association of these satellites to be better constrained.

The analysis of the distribution of the M31 subgroup reveals that the satellites are anisotropically distributed along our line of sight to M31, and the satellite system as a whole is skewed relative to its host in the direction of the Galaxy/Local Group barycentre. It is possible that this result might be due to distance errors or selection effects, but such explanations would require unlikely fine-tuning and the former explanation in particular has potentially significant consequences for the reliability and use of the main distance indicators. Some possible dynamical explanations are suggested but present problems due to the timescales involved. It may be that many of the M31 satellites were accreted into M31's halo only relatively recently. Alternatively, it is possible that the asymmetric satellite distribution that we observe is related to similar findings by van den Bosch et al. (2005) at higher redshift, and that this may be evidence to suggest that the halo of M31 is not yet virialised. However, until an adequate explanation for this distribution is presented, this finding warns against assuming that the M31 subgroup represents a complete, relaxed and unbiased population of galaxies.

ACKNOWLEDGEMENTS

We would like to thank Rodrigo Ibata, Geraint Lewis, Annette Ferguson and Nial Tanvir for help and discussions during the preparation of this work. AWM would like to thank Mark Wilkinson, Justin Read, Neil Wyn-Evans, Neil Trentham and Donald Lynden-Bell for enjoyable and useful discussions of these results. Thanks also go to Beth Willman, for her feedback on an earlier draft, and the anonymous referee, for a very useful and thorough report.

REFERENCES

Abadi, M. G., Navarro, J. F., & Steinmetz, M. 2005, astro-ph/0506659
Armandroff, T. E., Davies, J. E., & Jacoby, G. H. 1998, AJ, 116, 2287
Armandroff, T. E., Jacoby, G. H., & Davies, J. E. 1999, AJ, 118, 1220
Brainerd, T. G. 2005, ApJ, 628, L101
Brown, T. M., Ferguson, H. C., Smith, E., Kimble, R. A., Sweigart, A. V., Renzini, A., & Rich, R. M. 2004, AJ, 127, 2738
Bullock, J. S. & Johnston, K. V. 2004, astro-ph/0401625
Bullock, J. S., Kravtsov, A. V., & Weinberg, D. H. 2000, ApJ, 539, 517
Chapman, S. C., Ibata, R., Lewis, G. F., Ferguson, A. M. N., Irwin, M., McConnachie, A., & Tanvir, N. 2005, ArXiv Astrophysics e-prints
de Vaucouleurs, G. 1958, ApJ, 128, 465
Dekel, A. & Silk, J. 1986, ApJ, 303, 39
Dinescu, D. I., Keeney, B. A., Majewski, S. R., & Girard, T. M. 2004, AJ, 128, 687
Durrell, P. R., Harris, W. E., & Pritchet, C. J. 2001, AJ, 121, 2557
Einasto, J. & Lynden-Bell, D. 1982, MNRAS, 199, 67
Evans, N. W. & Wilkinson, M. I. 2000, MNRAS, 316, 929
Evans, N. W., Wilkinson, M. I., Guhathakurta, P., Grebel, E. K., & Vogt, S. S. 2000, ApJ, 540, L9
Fardal, M. A., Babul, A., Geehan, J. J., & Guhathakurta, P. 2005, astro-ph/0501241
Ferguson, A. M. N., Irwin, M. J., Ibata, R. A., Lewis, G. F., & Tanvir, N. R. 2002, AJ, 124, 1452
Freedman, W. L. & Madore, B. F. 1990, ApJ, 365, 186
Hoaglin, D. C., Mosteller, F., & Tukey, J. W. 1983, Understanding robust and exploratory data analysis (Wiley Series in Probability and Mathematical Statistics, New York: Wiley, 1983, edited by Hoaglin, David C.; Mosteller, Frederick; Tukey, John W.)
Holmberg, E. 1969, Ark. Astron., 5, 305
Ibata, R., Chapman, S., Ferguson, A. M. N., Irwin, M., Lewis, G., & McConnachie, A. 2004, MNRAS, 351, 117
Ibata, R., Chapman, S., Ferguson, A. M. N., Lewis, G., Irwin, M., & Tanvir, N. 2005, astro-ph/0504164
Ibata, R., Irwin, M., Lewis, G., Ferguson, A. M. N., & Tanvir, N. 2001, Nature, 412, 49
Irwin, M., Ferguson, A., Ibata, R., Lewis, G., & Tanvir, N. 2005, astro-ph/0505077
Irwin, M. J. 1994, in Dwarf Galaxies, 27
Irwin, M. J., Bunclark, P. S., Bridgeland, M. T., & McMahon, R. G. 1990, MNRAS, 244, 16P
Joshi, Y. C., Pandey, A. K., Narasimha, D., Sagar, R., & Giraud-Héraud, Y. 2003, A&A, 402, 113
Kahn, F. D. & Woltjer, L. 1959, ApJ, 130, 705
Karachentsev, I. D. & Karachentseva, V. E. 1999, A&A, 341, 355
Kauffmann, G., White, S. D. M., & Guiderdoni, B. 1993, MNRAS, 264, 201
Klypin, A., Zhao, H., & Somerville, R. S. 2002, ApJ, 573, 597
Knebe, A., Gill, S. P. D., Gibson, B. K., Lewis, G. F., Ibata, R. A., & Dopita, M. A. 2004, ApJ, 603, 7
Kochanek, C. S. 1996, ApJ, 457, 228
Kroupa, P., Theis, C., & Boily, C. M. 2005, A&A, 431, 517
Libeskind, N. I., Frenk, C. S., Cole, S., Helly, J. C., Jenkins, A., Navarro, J. F., & Power, C. 2005, astro-ph/0503400
Little, B. & Tremaine, S. 1987, ApJ, 320, 493
Lynden-Bell, D. 1976, MNRAS, 174, 695
—. 1981, The Observatory, 101, 111
—. 1982, The Observatory, 102, 202
Lynden-Bell, D. & Lynden-Bell, R. M. 1995, MNRAS, 275, 429
Majewski, S. R. 1994, ApJ, 431, L17
Martin, N. F., Ibata, R. A., Bellazzini, M., Irwin, M. J., Lewis, G. F., & Dehnen, W. 2004, MNRAS, 348, 12
Mateo, M. L. 1998, ARA&A, 36, 435
Mathewson, D. S., Cleary, M. N., & Murray, J. D. 1974, ApJ, 190, 291
McConnachie, A., Ferguson, A., Huxor, A., Ibata, R., Irwin, M., Lewis, G., & Tanvir, N. 2004a, The Newsletter of the Isaac Newton Group of Telescopes (ING Newsl.), issue no. 8, p. 8., 8, 8

McConnachie, A. & Irwin, M. J. 2005a, in IAU Colloquium 198
McConnachie, A. W. & Irwin, M. J. 2005b, MNRAS, submitted
McConnachie, A. W., Irwin, M. J., Ferguson, A. M. N., Ibata, R. A., Lewis, G. F., & Tanvir, N. 2004b, MNRAS, 350, 243
—. 2005, MNRAS, 356, 979
McConnachie, A. W., Irwin, M. J., Ibata, R. A., Ferguson, A. M. N., Lewis, G. F., & Tanvir, N. 2003, MNRAS, 343, 1335
McConnachie, A. W., Irwin, M. J., Lewis, G. F., Ibata, R. A., Chapman, S. C., Ferguson, A. M. N., & Tanvir, N. R. 2004c, MNRAS, 351, L94
Piatek, S., Pryor, C., Bristow, P., Olszewski, E., Harris, H., Mateo, M., Minniti, D., & Tinney, C. 2005, astro-ph/0503620
Piatek, S., Pryor, C., Olszewski, E. W., Harris, H. C., Mateo, M., Minniti, D., Monet, D. G., Morrison, H., & Tinney, C. G. 2002, AJ, 124, 3198
Schlegel, D. J., Finkbeiner, D. P., & Davis, M. 1998, ApJ, 500, 525
Schweitzer, A. E. 1996, Ph.D. Thesis
van den Bergh, S. 1972a, ApJ, 178, L99
—. 1972b, ApJ, 171, L31
—. 1974, ApJ, 191, 271
—. 1998, AJ, 116, 1688
van den Bosch, F. C., Weinmann, S. M., Yang, X., Mo, H. J., Li, C., & Jing, Y. P. 2005, astro-ph/0502466
Whiting, A. B., Hau, G. K. T., & Irwin, M. 1999, AJ, 118, 2767
Whiting, A. B., Irwin, M. J., & Hau, G. K. T. 1997, AJ, 114, 996
Wilkinson, M. I. & Evans, N. W. 1999, MNRAS, 310, 645
Willman, B., Dalcanton, J. J., Martinez-Delgado, D., West, A. A., Blanton, M. R., Hogg, D. W., Barentine, J. C., Brewington, H. J., Harvanek, M., Kleinman, S. J., Krzesinski, J., Long, D., Neilsen, E. H., Jr., Nitta, A., & Snedden, S. A. 2005, astro-ph/0503552
Willman, B., Governato, F., Dalcanton, J. J., Reed, D., & Quinn, T. 2004, MNRAS, 353, 639
Yang, X., Mo, H. J., van den Bosch, F. C., & Jing, Y. P. 2005, MNRAS, 356, 1293
Zaritsky, D., Smith, R., Frenk, C. S., & White, S. D. M. 1997, ApJ, 478, L53
Zentner, A. R., Kravtsov, A. V., Gnedin, O. Y., & Klypin, A. A. 2005, astro-ph/0502496
Zucker, D. B., Kniazev, A. Y., Bell, E. F., Martínez-Delgado, D., Grebel, E. K., Rix, H., Rockosi, C. M., Holtzman, J. A., Walterbos, R. A. M., Annis, J., York, D. G., Ivezić, Ž., Brinkmann, J., Brewington, H., Harvanek, M., Hennessy, G., Kleinman, S. J., Krzesinski, J., Long, D., Newman, P. R., Nitta, A., & Snedden, S. A. 2004, ApJ, 612, L121